Industria y Comercio
SUPERINTENDENCIA

Prosperidad para todos

SUPERINTENDENCIA DE INDUSTRIA Y COMERCIO	
RAD: 10-89491- -5	**FECHA**: 2012-11-20 15:39:05
DEP: 2020 DIRECCION DE NUEVAS CREACIONES	**EVE:** 378 FASE NACIONAL INCLUIDO CAPITULO I
TRA: 11 PCT-PATENTE DE INVENCION CAPITULOS I Y II	**FOLIOS**: 21
ACT: 519 PRESENTACION	

DIRECCIÓN DE NUEVAS CREACIONES

2020
Bogotá, D.C.,

Abogado(a)/Señor(a)
LUZ CLEMENCIA DE PAEZ
CAVELIER@CAVELIER.COM

Asunto: Radicación: 10-89491- -5
Trámite: 11
Evento: 378
Actuación: 519
Oficio: 21352
Folios: 21

Patente de Invención	X			Patente de Modelo de Utilidad	
Vía Nacional					
Vía PCT (Fase Nacional)	X	Capítulo I	X	Capítulo II	
No. Solicitud Internacional	PCT/US2009/031683				
Fecha de Presentación Internacional	22/01/2009				

Como resultado del Examen de Fondo realizado, con fundamento en el Artículo 45 de la Decisión 486 de la Comisión de la Comunidad Andina, se comunica:

1. **Documentos estudiados**

Descripción:	Folios 164 a 315	22/Julio/2010
Reivindicaciones:	Folios 316 a 347	22/Julio/2010
	Folios 403 a 411	10/Noviembre/2011
Prioridad:	US 61/011,799	22/Enero/2008
	US 61/115,297	17/Noviembre/2008

2. **Análisis de la Prioridad**

Se acepta la reivindicación de Prioridad porque esta solicitud fue presentada dentro del plazo establecido (Art. 9 D 486) y su contenido técnico corresponde con el de la prioridad reivindicada.

3. **Objeto de la invención**

De acuerdo con lo establecido en el numeral 1.2.2.2 del capitulo primero del Titulo 10 de la Circular Única para efectos del examen de patentabilidad, se tendrá en cuenta la tasa pagada por el solicitante al momento de comenzar el examen para las reivindicaciones adicionales; esto es que cuando la solicitud contenga más de diez (10)

reivindicaciones y no se haya pagado la tasa complementaria, sólo se estudiarán las cubiertas por la tasa pagada.
Para el caso de la presente solicitud, al verificar la tasa pagada, todo el capitulo reivindicatorio presentado se tendrá en cuenta para realizar el examen de patentabilidad.

Título de la solicitud: “Derivados de pirimidina 5-fluoro como fungicidas”.

El problema planteado en esta solicitud es la necesidad de desarrollar fungicidas que puedan tener mejor desempeño, sean mas fáciles de utilizar y un menor costo.

Para resolver este problema técnico la solicitud en estudio proporciona un compuesto de la fórmula 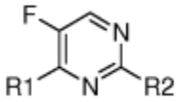

(I) donde los radicales están debidamente definidos (Fls. 165 – 178) como fungicidas.

El objeto de la presente Solicitud se relaciona con la Clasificación Internacional de Patentes (CIP): A 01 N 43/54 // P 3/00 // C 07 D 239/047 / 413/12.

4. De la Solicitud de Patente

Titulo

El título no corresponde con el objeto de la solicitud quizás porque se deba a una mala traducción, primero va la sustitución y luego el compuesto, por lo cual se sugiere al Solicitante hacer la corrección necesaria.

Reivindicaciones (Art 30 D 486, Art 22 PCT)

En la reivindicación 1 menciona la expresión: “opcionalmente” precediendo una característica por lo tanto no es concisa, porque hace opcional a las características y no permite delimitar el alcance de la reivindicación.

La reivindicación 1 no es concisa, porque presenta una excesiva complejidad puesto que cada uno de los radicales abarca una cantidad excesiva de definiciones de las cuales no existe una gran proporción que muestre actividad, lo cual dificulta determinar la extensión del objeto que se busca proteger.

5. Determinación del Estado de la Técnica

El Estado de la Técnica se determinó con base en la Fecha de Presentación de la Solicitud de Prioridad, Enero 22 de 2008 y se encontraron los siguientes documentos que anticipan el objeto de esta solicitud:

Ítem	Documento	Título	Fecha de Publicación*
D1	GB1461184	“Process for the manufacture of 5-fluorocytosine”	13/Enero/1977
D2	CA1254560	“N-(2-nitrophenyl)-4-aminopyrimidine derivatives, the preparation thereof and use thereof”	23/Mayo/1989
D3	Jaworski A. et Al, Journal of Molecular Structure, 223, pages 63-92, Elsevier Science	“Infrared spectra and tautomerism of b-fluoro-Cytosine, 5-bromocytosine and 5-iodocytosine. Matrix isolation and theoretical ab initio studies”	1990

	Publishers B.V., Amsterdam		

El documento D1 divulga (Pág. 1, líneas 13 – 22) que la 5-fluorocisteina es conocida como antimicótico, el cual es particularmente activo contra los organismos que causan candidiasis, criptococosis y cromoblastomicosis, se divulga el compuesto 2-etoxi-4-amino-5-fluoropirimidina de fórmula (I)

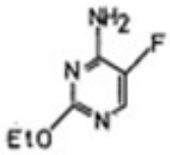

.

El documento D2 divulga (Págs. 40 y 41, reivindicación 1) el compuesto de fórmula

(I) 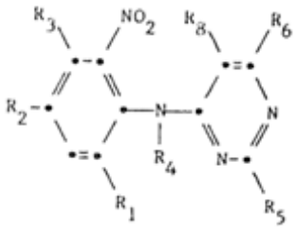

, donde R_1 es NO_2 o CF_3; R_2 es NO_2 o CF_3; R_3 es H o halógeno; R_4 es H o –C(O)R_7, en el cual R_7 es alquilo C_1-C_{12} sustituido o sin sustituir, entre otros; R_5, R6 y R8 es -O-R_{12}, entre otros, donde R_{12} es alquilo C_1-C_{12} sin sustituir o sustituido por halógeno, nitro, ciano, entre otros.

El documento D3 divulga (Fls. 418 – 432, Pág. 63; Pág. 67) que el 5-fluorocitosina y otros derivados 5-halogenados de citosina son importantes por su actividad anti-fúngica y anti-viral. Algunas de las funciones biológicas pueden estar relacionadas por el tautomerismo de la molécula . Dentro de los cuales se encuentra el 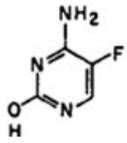

.

[1] URL: http://worldwide.espacenet.com/publicationDetails/biblio?DB=EPODOC&II=0&ND=3&adjacent=true&locale=en_EP&FT=D&date=19770113&CC=GB&NR=1461184A&KC=A

[2] URL:http://worldwide.espacenet.com/publicationDetails/biblio?DB=EPODOC&II=0&ND=3&adjacent=true&locale=en_EP&FT=D&date=19890523&CC=CA&NR=1254560A1&KC=A1

6. **Examen de Patentabilidad** (Art 14 D486)

Nivel Inventivo (Art18 D486)

La reivindicación 1 consiste en un compuesto de la fórmula general I 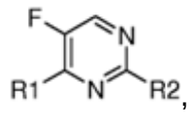

, donde los sustituyentes R^1, R^2 están debidamente definidos (folio 403 – 411)

Comparación de las características técnicas esenciales, con las del estado de la técnica:

Características esenciales	**D1 GB1461184**	**D2CA1254560**	**D3**
Compuesto de fórmula I 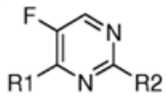	2-etoxi-4-amino-5-fluoropirimidina de fórmula (I) 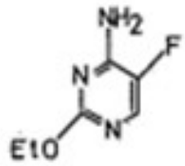	Un compuesto de fórmula I 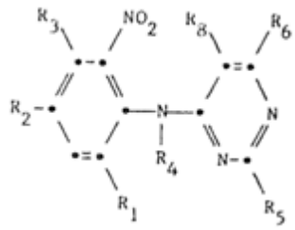	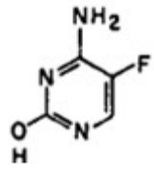
F	F	R8: halógeno	F
R^1: $-NR^3NR^4$, donde R^3 es H, alquilo C_1-C_6 o alquenilo C_2-C_6 sustituido con 1 a 3 R^5, un anillo heteroaromático tal como furanilo, pirazinilo, triazolilo, imidazol fusionado con un anillo aromático o heteroaromático, ciano, $-C(=O)R^6$, $-Si(R^8)_3$, entre otros; R^4 es H, alquilo C_1-C_6, opcionalmente sustituido con 1 a 3 R^5, $-C(=O)R^6$ o $-C(=O)N(R^8)R^{10}$; como alternativa R^3 y R^4 juntos forman un anillo saturado o insaturado de 5 ó 6 miembros que tiene 1 a 3 heteroátomos donde puede ser opcionalmente sustituido	H	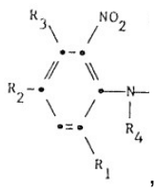 , donde R_1 es NO_2 o CF_3; R_2 es NO_2 o CF_3; R_3 es H o Halogeno; R_4 es H o $-C(O)R_7$, en el cual R_7 es alquil C_1-C_{12} sustituido o sin sustituir, entre otros	H
R^2: $-OR^{21}$, donde R^{21} es H, siempre que R^3 y R^4 ambos no sean igual a H, alquilo C_1-C_{14}, haloalquilo C_1-C_6, alquenilo C_2-C_4, entre otros	-OEt	R_5:-O-R_{12}, entre otros, donde R_{12} es alquilo C_1-C_{12} sin sustituir o sustituido por halógeno, nitro, ciano, entre otros	-OH

Los documentos del estado de la técnica cercanos a la invención corresponden a D1 D2 y D3 porque:

El documento D1 divulga que la 5-fluorocisteina es conocida como antimicótico, el cual es particularmente activo contra los organismos que causan candidiasis, criptococosis y cromoblastomicosis, se divulga el compuesto 2-etoxi-4-amino-5-fluoropirimidina de

fórmula (I) 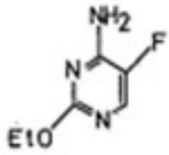 (Pág. 1, líneas 13 – 22)

El documento D2 divulga derivados de N-(2-nitrofenil)-4-aminopirimidina de fórmula (I), para el control de microorganismos no deseados en particular hongos fitopatógenos (Pág. 1, líneas 1 – 8). El compuesto de fórmula (I) 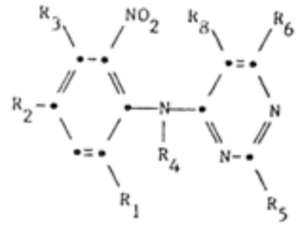 , donde R_1 es NO_2 o CF_3; R_2 es NO_2 o CF_3; R_3 es H o halógeno; R_4 es H o $–C(O)R_7$, en el cual R_7 es alquilo C_1-C_{12} sustituido o sin sustituir, entre otros; R_5, R6 y R8 es -O-R_{12}, entre otros, donde R_{12} es alquilo C_1-C_{12} sin sustituir o sustituido por halógeno, nitro, ciano, entre otros (Págs. 40 y 41, reivindicación 1)

El documento D3 divulga que el 5-fluorocitosina y otros derivados 5-halogenados de citosina son importantes por su actividad anti-fúngica y anti-viral. Algunas de las funciones biológicas pueden estar relacionadas por el tautomerismo de la molécula (folio 418, Pág. 63, introducción). Dentro de los cuales se encuentra el 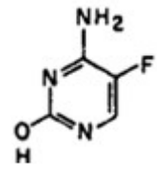 (folio 420, Pág. 67).

La diferencia entre la invención, definida en la reivindicación 1 y el compuesto del documento D1 consiste en que tiene un sustituyente mas, el grupo amino en la posición 4 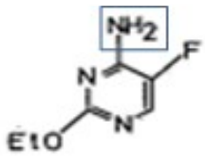 , mientras que para la solicitud en la posición 4 hay un H.

La diferencia entre la invención, definida en la reivindicación 1 y el compuesto del documento D2 consiste en que tiene un sustituyente mas, representado como R6 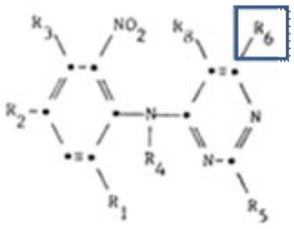 , mientras que para la solicitud en esa posición hay un H.

La diferencia entre la invención, definida en la reivindicación 1 y el compuesto del documento D3 consiste en que tiene un sustituyente mas, el grupo amino en la posición 4 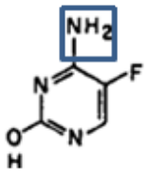

, mientras que para la solicitud en la posición 4 hay un H.

El efecto que lograría las diferencias antes mencionada en el compuesto de fórmula I de la reivindicación 1, en cuanto a su acción como fungicida, no puede ser determinado toda vez que no existe alguna evidencia que indique que dichas diferencias estructurales, otorgan al compuesto ahora reivindicado una ventaja técnica sobre los compuestos ya conocidos en la anterioridad D1 o D2 o D3.

Por lo tanto, el problema técnico objetivo a resolver consiste en plantear una alternativa a los compuestos de fórmula I conocidos según los documentos D1 o D2 o D3 para que sea más eficiente su actividad como fungicida.

Teniendo en cuenta lo expuesto anteriormente, la personas de nivel medio versada en la materia derivara de manera obvia los compuestos descritos en la reivindicación 1 de la presente invención a partir de las enseñanzas del documento D1 o D2 o D3 toda vez que las diferencias se limitan a variaciones en uno de los sustituyentes, sin que ese hecho confiera una mayor acción como fungicidas.

Conclusión:
La reivindicación 1 cumple el requisito de novedad (Art. 16), pero no cumplen con el requisito de nivel inventivo (Art. 18).

7. Conclusión

Los requisitos de Patentabilidad de la presente Solicitud están afectados así:

Ítem	Documento	Reivindicaciones afectadas	Requisito que afecta
D1	WO2004052280	1	Nivel Inventivo
D2	CA1254560	1	Nivel Inventivo
D3	Jaworski A. et Al, Journal of Molecular Structure, 223, pages 63-92, Elsevier Science Publishers B.V., Amsterdam	1	Nivel Inventivo

En cumplimiento del artículo 45 de la Decisión 486 de la Comisión de la Comunidad Andina, se le indica que debe dar respuesta dentro del término de sesenta (60) días contados a partir de la fecha de notificación de la presente comunicación. En caso de no dar respuesta al presente requerimiento, o si a pesar de la respuesta subsistieran los impedimentos para la concesión, se denegará la patente.

Se invita al solicitante se sirva indicar, si así lo considera, su renuncia al término faltante de sesenta (60) días para dar respuesta a este requerimiento y presentarla por escrito.

Finalmente, se le recuerda al solicitante que si como respuesta a este requerimiento llegara a modificar el capítulo reivindicatorio y éste contenga más de diez (10) reivindicaciones, no pagará la tasa de modificación voluntaria pero sí la correspondiente al pago por reivindicación adicional.

Notifíquese el presente oficio conforme a lo dispuesto en el numeral 5.2, literal e), del capítulo quinto del título primero de la Circular Única No. 10 de 2001.

JOSÉ LUIS SALAZAR LÓPEZ
Director de Nuevas Creaciones (c)

El anterior requerimiento fue notificado por fijación en lista, de fecha 2012-11-27

Elaboró: Mayra Alejandra Quintero
Revisó: Gloria Jacqueline Alfonso Rozo

Journal of Molecular Structure, 223 (1990) 63–92
Elsevier Science Publishers B.V., Amsterdam — Printed in The Netherlands

INFRARED SPECTRA AND TAUTOMERISM OF 5-FLUOROCYTOSINE, 5-BROMOCYTOSINE AND 5-IODOCYTOSINE. MATRIX ISOLATION AND THEORETICAL AB INITIO STUDIES*

ANDRZEJ JAWORSKI**, MARIAN SZCZESNIAK, KRYSTYNA SZCZEPANIAK, KUHALIM KUBULAT and WILLIS B. PERSON

Department of Chemistry, University of Florida, Gainesville, FL 32611 (U.S.A.)

(Received 30 May 1989)

ABSTRACT

The infrared (IR) spectra of 5-fluorocytosine (5FC), 5-bromocytosine (5BrC) and 5-iodocytosine (5IC) all isolated in an argon matrix at 15 K are presented and discussed. Vibrational assignments are proposed based on ab initio quantum mechanical calculations (3-21G basis set) of the IR frequencies and intensities for the amino-oxo and amino-hydroxy tautomers of 5FC. The IR spectra prove that the amino-hydroxy tautomer strongly dominates in an inert matrix for all the 5-halogenated cytosines studied, in sharp contrast with the dominance of the amino-oxo form in polar media. From the experimental absorbances and theoretical molar absorption coefficients the equilibrium constants. K(h/o), and the difference in the energies of the amino-hydroxy and amino-oxo tautomers are estimated. The value for 5FC agrees very well with the energy difference calculated using a 6-31G** basis set (single point) and 3-21G optimized geometry, corrected for the difference in the zero-point vibrational energy.

INTRODUCTION

Studies of the physicochemical properties of 5-fluorocytosine (5FC) and other 5-halogenated derivatives of cytosine are important not only for intrinsic reasons, but also because these molecules – particularly 5FC and its nucleoside – exhibit anti-tumor (anti-leukemia), anti-fungal and anti-viral activities (e.g. see [1–4] and references therein). Some of the biological functions of 5FC might be related to the tautomerism of this molecule.

The aims of this work were: (i) to determine the tautomeric equilibrium of 5-halogenated cytosines isolated in a hydrophobic inert matrix environment based on an analysis of the infrared (IR) spectrum; (ii) to perform an ab initio calculation of the vibrational spectrum (with a 3-21G basis set) and stabilization energy (with a 6-31G** basis set) of the amino-oxo and amino-hydroxy

*Dedicated to Professor E. Bright Wilson, Jr.
**On leave (1986–1987) from the Institute of Physics, Technical University, Warsaw, Poland.

0022-2860/90/$03.50 © 1990 Elsevier Science Publishers B.V.

tautomers of 5FC which were identified from the matrix spectrum; (iii) to interpret the IR spectrum of 5FC and other 5-halogenated cytosines on the basis of this calculation; and (iv) to analyse the effect of substitution of a different halogen at C5 and of intermolecular interactions on the tautomerism and IR spectrum of these molecules.

Studies of the IR spectra of isolated molecules are important because they provide the reference frequencies and intensities for comparison with the spectra of these molecules placed in any interacting environment; for example, in aqueous solution, crystalline solid or after incorporation into DNA or RNA (e.g. see ref. 5). Such comparison provides information about the effect of intermolecular interaction with each of these environments not only on the molecule as a whole, but also on each particular part of the molecule.

EXPERIMENTAL PROCEDURE

The IR spectra were recorded on a Nicolet model 7199 FTIR spectrometer. The experimental conditions and procedures used were the same as those described previously [6,7]. The samples of 5FC, 5-bromocytosine (5BrC) and 5-iodocytosine (5IC) were obtained from Sigma. With the exception of 5BrC the samples were used with no further purification except for the sublimation occurring as the sample was deposited into the matrix. The sample of 5BrC required additional purification, vacuum sublimation, before the matrix experiment was done. A deuterated sample of 5FC was prepared by repeated recrystallization of 5FC from D_2O solution. To prove that the compound did not decompose during heating, the IR spectrum of a solid film deposited during heating to the same temperature as for the matrix study was compared with the spectrum of an unheated crystalline sample (in KBr). Both spectra were found to be the same.

THEORETICAL CALCULATIONS

Geometry optimization for both the amino-oxo and the amino-hydroxy tautomers, and for all possible rotamers of these forms of 5FC, was performed using a 3-21G basis set [8a] with GAMESS [8b,c] and GAUSSIAN 82 [8d] systems of programs running on CDC CYBER 205 (with the former) and on CRAY/XMP48 (with the latter) computers. The geometries of the corresponding tautomers of cytosine obtained from references [6] and [8e] were used as a starting point. The frequency and intensity calculations with a 3-21G basis set, as well as one-point calculations with a 6-31G** basis set at the 3-21G optimized geometry (6-31G**//3-21G) [8f,g] were performed for the lowest-energy rotamers using the GAUSSIAN 82 program installed on the CRAY/XMP48 computer at the Pittsburgh Supercomputer Center, using an-

alytical first and second derivatives. Zero-point energies were obtained from frequencies calculated with the 3-21G basis set.

RESULTS OF EXPERIMENT AND CALCULATIONS

Molecular geometries

The frequency calculations confirm that for all considered tautomeric forms and their rotamers 5FC is essentially planar. The calculated geometries are given in Fig. 1. (The numbering of atoms is shown in Fig. 2.) The fluorine

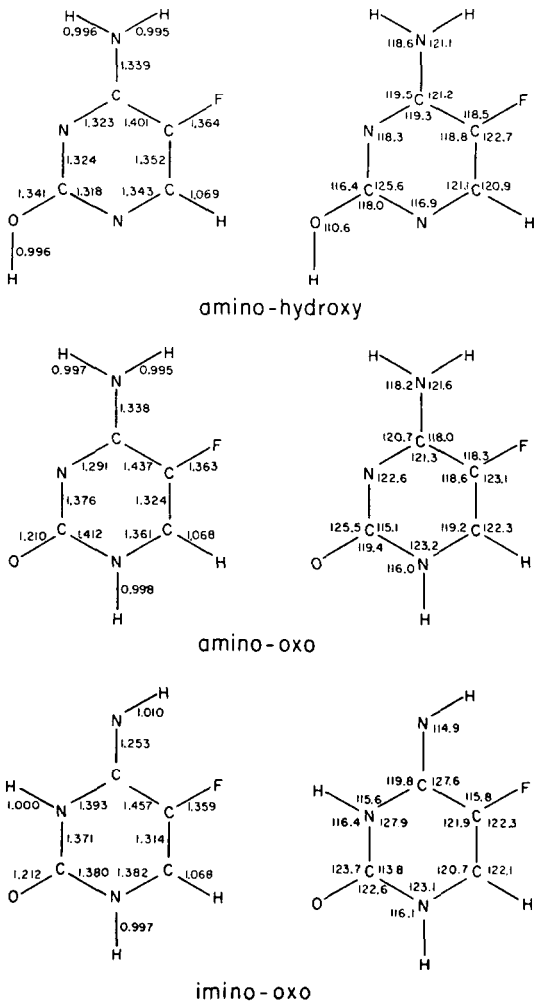

Fig. 1. Calculated (3-21G) optimized geometries (bond lengths and angles) for the amino-hydroxy, amino-oxo and imino-oxo tautomers of 5FC.

atom substitution in position 5 causes almost all bond lengths (except for C2–N3 and C6–N1) to become a bit shorter than in cystosine (for example, by 0.015 Å, 0.013 Å and 0.011 Å for the C5–C6 bond in the amino-hydroxy, amino-oxo and imino-oxo forms, respectively). The shortening of these bonds is similar to the effect observed for 5-fluorouracil by Scanlan and Hillier [8e]. The C2–N3 and C6–N1 bonds in 5FC are predicted to elongate by about half of these values in comparison with the bond lengths for similar forms of cytosine [6,8e].

The substitution of the fluorine atom at position 5 causes the NH_2 group to tilt in the direction of the fluorine (the N3–C4–N8 angle increases by more than 2°), a decrease in the C4–N8–H10 angle and a decrease in the C4–C5–F11 angle (more than 4° in comparison with the C4–C5–H11 angle in cytosine). As a result, the distance between the H10 proton of the NH_2 group and the F atom decreases, suggesting some kind of weak intramolecular hydrogen bond. The N8F distances are 2.75 Å, 2.71 Å and 2.82 Å for amino-hydroxy, amino-oxo and imino-oxo forms, respectively. The formation of these weak hydrogen bonds stabilizes the planar tautomeric forms considered here for 5FC.

The results of the calculations of the energies are presented in Table 1. On the 3-21G//3-21G level the amino-oxo form of 5FC is calculated to be lowest in energy; the amino-hydroxy tautomer and the imino-oxo tautomer are predicted to be higher in energy by 8.4 and 3.2 kJ mol^{-1}, respectively (with the vibrational corrections).

When calculations using a better basis set (6-31G**//3-21G) are performed: the order of the stability of the three tautomeric forms reverses. The total energy calculated with the 6-31G** basis at the global energy minimum of tautomers optimized at the 3-21G level is lowest for the amino-hydroxy form.

After including the zero-point vibrational energies, the amino-oxo form is predicted to be 13 kJ mol^{-1} and the imino-oxo form 15.2 kJ mol^{-1} less stable than the amino-hydroxy tautomer.

The amino-oxo form is predicted to have the largest dipole moment: 5.56 D at the 6-31G**//3-21G level. At the same level the dipole moment of the imino-oxo form is calculated to be 3.97 D, and the dipole moment of the amino-hydroxy tautomer 1.82 D. From the differences in these values one can predict a strong stabilization of the amino-oxo form in a polar environment. This effect could be responsible for the predominance of the amino-oxo tautomer in the crystal and in aqueous solutions [9].

Influence of electron correlation

High-level calculations on molecular fragments mimicking the different tautomeric forms of nucleic acid bases [10] have shown that, in the case of the hydroxy-oxo tautomerism of these systems, corrections to the energy for correlation contributions favor the hydroxy tautomer. This correction was found

TABLE 1

Total HF energies, zero-point vibrational energies, and relative energies for the three lowest tautomeric forms of 5-fluorocytosine

Level of calculation	Tautomeric form		
	Amino-oxo	Imino-oxo	Amino-hydroxy
3-21G//3-21G			
Global minimum (a.u.)	−488.73049	−488.72990	488.72630
Zero-point			
Vibrational energy (kJ mol^{-1})	260.20	261.86	257.61
Relative energy			
(kJ mol^{-1})	0[a]	+3.2	+8.4
6-31G**/3-21G			
Global minimum (a.u.)	−491.46681	−491.46620	−491.47077
6-31G**/3-21G			
Relative energy[b] (kJ mol^{-1})	+13.0	+16.2	0[a]

[a]The energy of the most stable tautomeric form is defined to be zero and the energies of the other forms relative to it are listed. [b]Zero-point vibrational energy from the 3-21G//3-21G level.

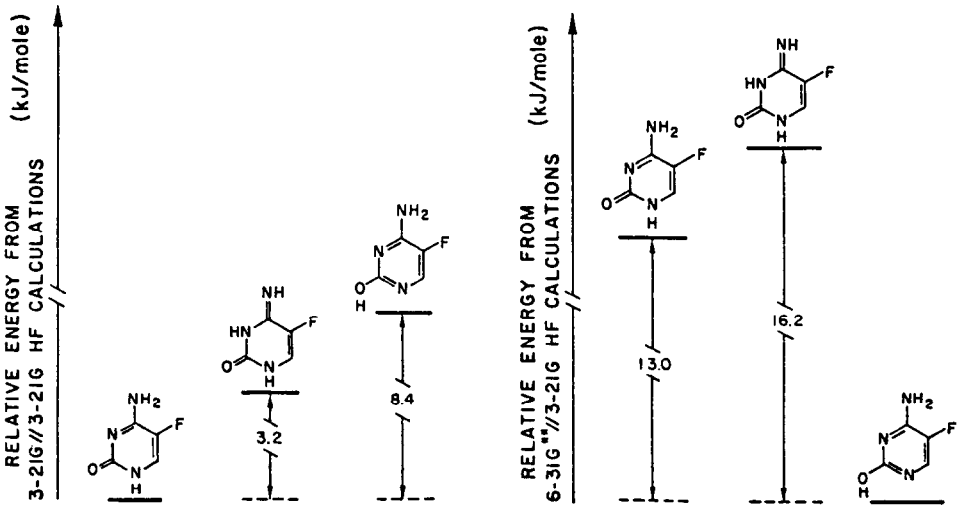

to be especially significant for cytosine, although it was not important for uracil tautomers. In the case of the amino-imino tautomers of the pyrimidines the electron-correlation effects favor the amino forms. However, calculations by Les et al. [11] on the entire cytosine molecule using the OVOS method [12]

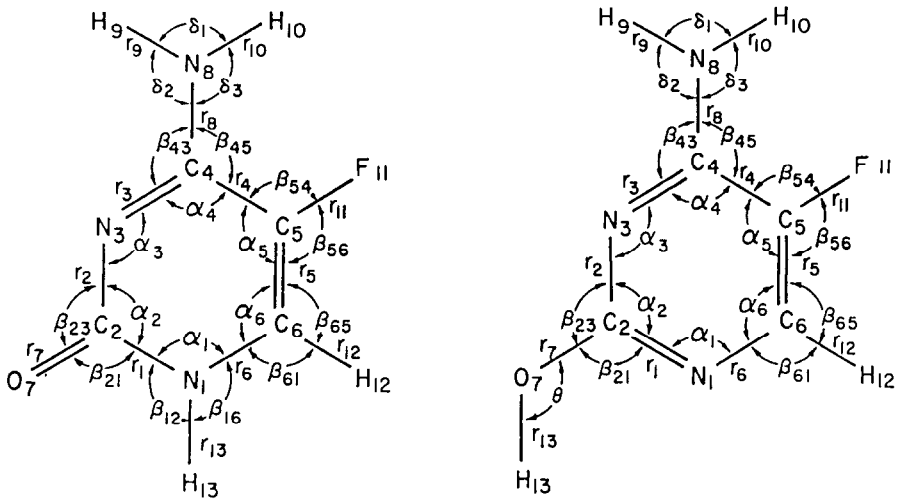

Fig. 2. Definition of internal coordinates for amino-oxo and amino-hydroxy tautomers of 5FC.

showed that higher-order correlation corrections almost exactly cancel the extra stabilization of the amino-hydroxy form resulting from the second-order MBPT correction [13]. The results of Kwiatkowski et al. [10] and of Les et al. [11] allow us to assume that even at the highest correlation level the amino-hydroxy form of the isolated 5FC molecule will still be predicted to be the most stable form, in agreement with the results obtained here on the HF level for the 6-31G* basis set.

IR spectra

The 5FC molecule has 13 atoms in C_s symmetry with 33 normal modes of vibrations: 10 out-of-plane and 23 in-plane modes. The symmetry-coordinate definition is given in Fig. 2 and in Table 2 and the calculated diagonal force constants are collected in Table 3. The use of published scaling procedures [14,15] with a number of scaling factors seemed to be unsuitable for the ab initio calculation on a large molecule with a very complicated IR spectrum, where the unequivocal assignment of the observed spectrum to calculated normal vibrations is not an easy problem. We decided to use a uniform scaling factor of 0.91 for the calculated in-plane frequencies and another value (0.81) for the out-of-plane frequencies (see footnote b in Table 5). For the OH stretch a factor of 0.92 was used, in accordance with the experimental and theoretical studies on other related molecules, e.g. 2-hydroxypyrimidine [16].

TABLE 2

Symmetry coordinates of the 5FC tautomers for the description of vibrational modes

Symmetry coordinate	Description[a]
In-plane	
$S_1 = \Delta r_1$	N1C2 stretching
$S_2 = \Delta r_2$	C2N3 stretching
$S_3 = \Delta r_3$	N3C4 stretching
$S_4 = \Delta r_4$	C4C5 stretching
$S_5 = \Delta r_5$	C5C6 stretching
$S_6 = \Delta r_6$	C6N1 stretching
$S_7 = \Delta r_7$	C2O7 stretching
$S_8 = \Delta r_8$	C4N8 stretching
$S_9 = \Delta r_9$	N8H9 stretching
$S_{10} = \Delta r_{10}$	N8H10 stretching
$S_{11} = \Delta r_{11}$	C5F stretching
$S_{12} = \Delta r_{12}$	C6H stretching
$S_{13} = \Delta r_{13}$	N1H stretching, in oxo
	OH stretching, in hydroxy
$S_{14} = 1/\sqrt{6}(\Delta\alpha_1 - \Delta\alpha_2 + \Delta\alpha_3 - \Delta\alpha_4 + \Delta\alpha_5 - \Delta\alpha_6)$	Ring def. 1
$S_{15} = 1/\sqrt{12}(2\Delta\alpha_1 - \Delta\alpha_2 - \Delta\alpha_3 + 2\Delta\alpha_4 - \Delta\alpha_5 - \Delta\alpha_6)$	Ring def. 2
$S_{16} = 1/2(\Delta\alpha_2 - \Delta\alpha_3 + \Delta\alpha_5 - \Delta\alpha_6)$	Ring def. 3
$S_{17} = 1/\sqrt{2}(\Delta\beta_{21} - \Delta\beta_{23})$	C2O7 bending
$S_{18} = 1/\sqrt{2}(\Delta\beta_{43} - \Delta\beta_{45})$	C4N8 bending
$S_{19} = 1/\sqrt{2}(\Delta\beta_{54} - \Delta\beta_{56})$	C5F bending
$S_{20} = 1/\sqrt{2}(\Delta\beta_{65} - \Delta\beta_{61})$	C6H bending
$S_{21} = 1/\sqrt{2}(\Delta\beta_{12} - \Delta\beta_{16})$ oxo	N1H bending (in oxo form)
$S_{21} = \Delta\theta$ hydroxy	O7H13 bending (in hydroxy form)
$S_{22} = 1/\sqrt{6}(2\Delta\delta_1 - \Delta\delta_2 - \Delta\delta_3)$	NH_2 scissoring
$S_{23} = 1/\sqrt{2}(\Delta\delta_2 - \Delta\delta_3)$	NH_2 rocking
Out-of-plane	
$S_{24} = \Delta\gamma_2$	C2O OOPL wagging
$S_{25} = \Delta\gamma_4$	C4N8 OOPL wagging
$S_{26} = \Delta\gamma_5$	C5F OOPL wagging
$S_{27} = \Delta\gamma_6$	C6H OOPL wagging
$S_{28} = \Delta\gamma_1$ oxo	N1H OOPL wagging (in oxo form)
$S_{28} = \Delta\tau_{OH}$ hydroxy	OH torsion (in hydroxy form)
$S_{29} = \Delta\tau_{N8H9}$	N8H9 torsion
$S_{30} = \Delta\tau_{N8H10}$	N8H10 torsion
$S_{31} = 1/\sqrt{6}(\Delta\tau_{12} - \Delta\tau_{23} + \Delta\tau_{34} - \Delta\tau_{45} + \Delta\tau_{56} - \Delta\tau_{61})$	OOPL ring def. 1
$S_{32} = 1/\sqrt{2}(\Delta\tau_{12} - \Delta\tau_{34} + \Delta\tau_{45} - \Delta\tau_{61})$	OOPL ring def. 2
$S_{33} = 1/\sqrt{12}(-\Delta\tau_{12} + 2\Delta\tau_{23} - \Delta\tau_{34} - \Delta\tau_{45} + 2\Delta\tau_{56} - \Delta\tau_{61})$	OOPL ring def. 3

[a]Abbreviations: OOPL, out of plane; def., deformation.

TABLE 3

Diagonal elements of 5FC in internal coordinates (in mdyn $Å^{-1}$)

5-Fluorocytosine (hydroxy-amino)			5-Fluorocytosine (keto-amino)		
Internal coordinate no.		Force constant	Internal coordinate no.		Force constant
	In plane			*In plane*	
	Stretching			*Stretching*	
1	N1-C2	8.7923	1	N1-C2	5.6651
2	C2-N3	8.5553	2	C2-N3	6.7462
3	N3-C4	8.7539	3	N3-C4	10.3595
4	C4-C5	7.1635	4	C4-C5	6.1910
5	C5-C6	8.9534	5	C5-C6	10.6210
6	C6-N1	7.8204	6	C6-N1	7.5594
7	C2-O7	7.7000	7	C2-O7	14.1236
8	C4-N8	8.3177	8	C4-N8	8.3631
9	N8-H9	8.2121	9	N8-H9	8.1797
10	N8-H10	8.2658	10	N8-H10	8.2638
11	C5-F11	7.5814	11	C5-F11	7.6314
12	C6-H12	6.3701	12	C6-H12	6.4081
13	O7-H13	8.5290	13	N1-H13	8.0430
	Bending			*Bending*	
14	C2-N1-C6	0.8551	14	C2-N1-C6	0.8675
15	N1-C2-N3	0.9505	15	N1-C2-N3	0.9031
16	C2-N3-C4	0.8203	16	C2-N3-C4	0.7332
17	N3-C4-C5	0.8625	17	N3-C4-C5	0.8232
18	C4-C5-C6	0.9659	18	C4-C5-C6	0.9298
19	C5-C6-N1	0.8282	19	C5-C6-N1	0.8042
20	C2-O7-H13	0.9249	20	C6-N1-H13	0.3173
21	N1-C2-O7	0.6793	21	C2-N1-H13	0.3173
22	N3-C2-O7	0.6793	22	N1-C2-O7	0.6861
23	N3-C4-N8	0.5918	23	N3-C2-O7	0.6861
24	C5-C4-N8	0.5918	24	N3-C4-N8	0.6378
25	C4-C5-F11	0.4779	25	C5-C4-N8	0.6378
26	C6-C5-F11	0.4779	26	C4-C5-F11	0.4916
27	C5-C6-H12	0.3223	27	C6-C5-F11	0.4916
28	N1-C6-H12	0.3223	28	C5-C6-H12	0.3098
29	H9-N8-H10	0.3876	29	N1-C6-H12	0.3098
30	C4-N8-H9	0.4356	30	H9-N8-H10	0.3878
31	C4-N8-H10	0.4430	31	H9-N8-C4	0.4479
			32	H10-N8-C4	0.4479
	Out-of-plane wag			*Out-of-plane wag*	
32	O7-C2-N1-N3	0.8794	33	H13-N1-C2-C6	0.3061
33	N8-C4-N3-C5	0.9690	34	O7-C2-N1-N3	1.0294

5-Fluorocytosine (hydroxy-amino)			5-Fluorocytosine (keto-amino)		
Internal coordinate no.		Force constant	Internal coordinate no.		Force constant
34	F11-C5-C4-C6	0.8054	35	H13-N1-C2-C6	0.3061
35	H12-C6-N1-C5	0.6607	36	O7-C2-N1-N3	1.0294
			37	N8-C4-N3-C5	0.9258
				F11-C5-C4-C6	0.7811
				H12-C6-N1-C5	0.6306
	Torsion			*Torsion*	
36	H13-O7-C2-N1	0.0345	38	N1-C2-N3-C4	0.0954
37	H13-O7-C2-N3	0.0345	39	C2-N3-C4-C5	0.1185
38	H9-N8-C4-N3	0.0377	40	N3-C4-C5-C6	0.1769
39	H9-N8-C4-C5	0.0377			
40	H10-N8-C4-N3	0.0323			
	Torsion			*Torsion*	
41	H10-N8-C4-C5	0.0323	41	C4-C5-C6-N1	0.2388
42	N1-C2-N3-C4	0.1410	42	C5-C6-N1-C2	0.1826
43	C2-N3-C4-C5	0.1550	43	C6-N1-C2-N3	0.0977
44	N3-C4-C5-C6	0.1947	44	N9-N8-C4-N3	0.0449
45	C4-C5-C6-N1	0.2204	45	H9-N8-C4-C5	0.0449
46	C5-C6-N1-C2	0.1820	46	H10-N8-C4-N3	0.0345
47	C6-N1-C2-N3	0.1423	47	H10-N8-C4-C5	0.0345

EXPERIMENTAL RESULTS AND DISCUSSION

The tautomeric equilibria of the substituted cytosines studied here can be examined most convincingly by analysis of the spectral region related to the characteristic stretching vibrations of the OH, NH and C=O groups directly involved in the tautomeric transition. This part of the IR spectra of 5FC, 5BrC, 5IC and, for comparison, cytosine, is shown in Fig. 3 for the molecules isolated in argon matrices. The most important findings from these spectra are: (i) the appearance in each spectrum of a relatively strong absorption from the OH stretching mode near 3600 cm^{-1} (see results for model systems e.g. refs. 16,17) related to the amino-hydroxy tautomer; (ii) the presence in the spectra of all 5-halogenated cytosines of only trace absorption by the N1H stretching mode near 3470–3460 cm^{-1} (see results for model systems, e.g. [18]) related to the

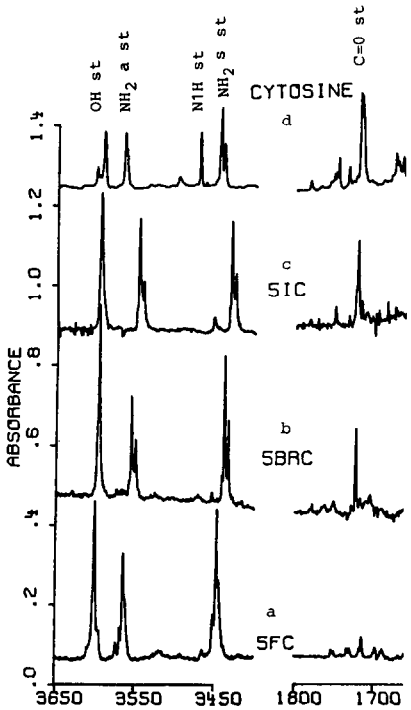

Fig. 3. IR spectra in the OH, NH and C=O stretching regions of 5FC (a), 5BrC (b), 5IC (c) and cytosine (d), each isolated in an argon matrix at about 15 K.

amino-oxo tautomer; (iii) the appearance in the spectrum of 5FC of only trace absorption by the C=O stretching mode near 1710–1750 cm^{-1} (see results for model systems, e.g. ref. 18) related also to the amino-oxo tautomer. It is clear that the hydroxy tautomer is predominant.

From the ratio of experimental absorbances of the OH stretching modes to those for the C=O (or N1H) stretches it was possible to determine the oxo⇌hydroxy equilibrium constant

$$K(\mathrm{h/o}) = [\mathrm{h}]/[\mathrm{o}] = [\mathrm{abs(OH)/abs(C{=}O)}] * [A(\mathrm{C{=}O})/A(\mathrm{OH})] \quad (1)$$

or

$$K(\mathrm{h/o}) = [\mathrm{abs(OH)/abs(N1H)}] * [A(\mathrm{N1H})/A(\mathrm{OH})] \quad (2)$$

where [h] is the concentration of hydroxy form, [o] the concentration of oxo form, abs(OH), abs(C=O) and abs(N1H) are the experimentally measured integrated absorbances and A(OH), A(C=O) and A(N1H) are the calculated molar absorption coefficients.

Because the observed absorbance is very low for the N1H bands of halogen-

ated cytosines and so cannot be determined accurately, we have used only eqn. (1) to estimate $K(\mathrm{h/o})$.

We believe that this value for the equilibrium constant $K(\mathrm{h/o})$ reflects the equilibrium as it exists in the gas phase at about 500 K, just before the compound is codeposited together with the Ar matrix gas onto the cold window in the matrix experiment. From this equilibrium constant at $T=500$ K, we may estimate the value for the standard Gibbs free energy difference as

$$\Delta G_{\mathrm{T}}^{0}(\exp) = -RT \ln K(\mathrm{h/o}) \tag{3}$$

We expect that the entropies of the amino-hydroxy and amino-oxo forms are similar [19] so that the entropy difference is approximately zero and $\Delta G^{0} \simeq \Delta H^{0}$. The difference between ΔH_{500}° and ΔE_{0}° may also be expected to be relatively small, and we neglect it in the following discussion.

Table 4 summarizes the $K(\mathrm{h/o})$ and ΔH_{500}° values for all cytosines studied here. The calculated values for the differences in the stabilization energies (ΔE_{0}° (calc)) are known only for cytosine and for 5FC [11,13,21]. These values are given in the last column of Table 4.

For all the cytosine derivatives listed in Table 4 the amino-hydroxy tautomer is favored over the amino-oxo form, but the magnitudes of the ΔH values gradually increase on going from cytosine to 5IC, to 5BrC and, finally, to 5FC. Such an increase in the relative stabilities of the tautomeric forms can be correlated with the changes of the electronegativities of the atom attached to C5 (see, for example, ref. 20).

The agreement between the experimentally determined value of ΔH of 5FC and the calculated value of ΔE_{0}° (3-21G//6-31G**) is surprisingly good, as is the agreement with the slightly higher value calculated recently at the coupled cluster level [21].

The same order of agreement between the experimental and calculated energy differences was also found for cytosine. For both 5FC and cytosine, the

TABLE 4

Experimental equilibrium constants, $K(\mathrm{h/o})$, and enthalpy differences, ΔH, compared with the calculated stabilization energy differences, ΔE_{0}°, for isolated cytosines

Compound	$K(\mathrm{h/o})$[f]	$\Delta H_{\mathrm{T}}^{\circ}$[f] (kJ mol^{-1})	ΔE_{0}° (kJ mol^{-1})
Cytosine	2.5[a]	−4	−1[b]; −4[c]
5IC	8.4	−8	
5BrC	12.5	−11	
5FC	21.8	−13	−13[d]; −21.7[e]

[a]Estimated from the data in our previous work [6] (also on the basis of OH and total C=O absorption bands). [b]From ref. 13. [c]From ref. 11. [d]This work. [e]From ref. 21. [f]The estimated error in these values is about 30%.

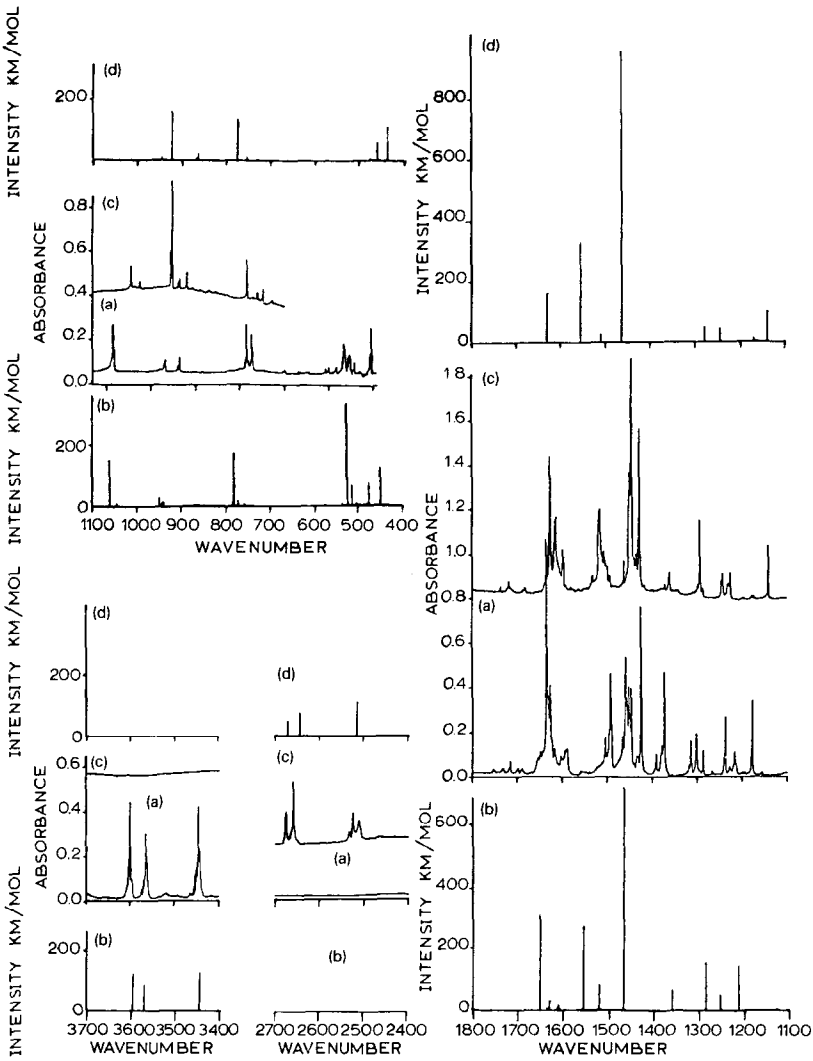

Fig. 4. Comparison of the experimental IR spectra of 5FC (a) and its deuterated analog (c) with the corresponding calculated spectra of the amino-hydroxy tautomer of 5FC (b) and its deuterated analog (d).

experimental and the calculated results both show that the isolated amino-hydroxy tautomer is more stable.

Comparison of experimental and calculated IR spectra of 5FC

A comparison of the experimental IR spectrum of 5FC isolated in an argon matrix, where it is found predominantly in the amino-hydroxy tautomeric form,

TABLE 5

Vibrational frequencies, ν, infrared intensities, A, and assignments of the absorption bands of isolated 5FC

Experimental (Ar)		Calculation				Additional experimental bands; assignment[d]
ν (cm^{-1})	A (rel)[a]	ν^b (cm^{-1}) Scaled	ν^b (cm^{-1}) Unscaled	A (km mol^{-1})	PED[c,d]	
3602	110	3592	3905	126	OH str. (100)	
3573	20					ROT
3568	25					ROT
3564	74	3564	3916	90	NH_2 asym.str. (100)	
3520	9					Ass
3465	9					N1H str./o
3452	32					ROT
3448	104	3447	3788	130	NH_2 sym.str. (100)	
3445	56					MS
Not visible		3104	3411	4	C6H str. (99)	
1754	4					
1750	3					FR/o
1733	5					MS/o
1730	5					
1715	14					C=O str./o
1699	11					Ass/o
1689	9					
1653	21					FR: e.g. 1177 + 487 = 1664
1649	27					1155 + 487 = 1642
1644	21					ROT
1634	268	1648	1811	312	NH_2 sc. (74)	
1627	74	1628	1789	22	C5C6 str. (30+), NH_2 sc. (18−)	
1617	30					FR: 1177 + 446 = 1623
1602	30					1237 + 373 = 1610
1593	29					1115 + 446 = 1601
1588	30					1342 + 253 = 1580
1503	45					FR: e.g. 938 + 565 = 1503
1492	115	1570	1726	273	C4C5 str. (30−), N1C2 str. (18−)	
1465	24					FR: 1155 + 317 = 1472
1458	133	1522	1673	86	C-O str. (23+), RI def.1 (16−), C4N8 str. (15+), C2N3 str. (14−)	

TABLE 5 (continued)

Experimental (Ar)		Calculation				Additional experimental bands; assignment[d]
ν (cm^{-1})	A (rel)[a]	ν^b (cm^{-1}) Scaled	ν^b (cm^{-1}) Unscaled	A (km mol^{-1})	PED[c,d]	
1455	88					FR: e.g. 1177+287=1464 968+487=1455 1155+287=1442
1448	70					
1445	99					
1438	14					
1433	23					
1431	23					
1425	50					FR: 1177+253=1430
1423	192	1480	1627	718	N3C4 str.(24−), C4N8 str.(20+), N1C2 str.(12+)	
1390	25					FR: e.g. 1085+330=1415 1085+317=1402
1378	36					
1372	117	1359	1494	69	C5C6str.(19+), N1C6 str.(18+), C6H bend.(15+), OH bend.(11+)	
1354	5					
1317	12					MS
1313	39	1296	1424	156	C6H bend.(51−), OH bend.(14+)	
1285	32					FR: e.g. 700+585=1285
1265	6					
1237	68	1264	1389	49	CF str.(33−), NH_2 rock.(16+), RI def.1(16−)	
1227	12					
1216	29					FR:e.g.968+287
1177	86	1210	1345	145	OH bend.(32+), N1C6 str.(26−), NH rock.(14+)	
1155	6	1124	1249	4	C2N3 str.(26+), N1C2 str.(18−), N1C6 str.(18+)	
1085	60	1059	1176	152	NH_2 rock.(31−), N3C4 str.(21+), OH bend.(13+)	
968	16	957	1052	28	N1C2 str.(26+), RI def.1(16−), NH_2 rock.(13−), C2N3 str.(12+)	
940	6					MS
938	20	938	1158	12	C6H OOPL wag.(100)	
785	60	787	965	171	RI def.1 OOPL(48+), C4N8 OOPL wag.(31+), C-O OOPL wag.(18+)	
780	16	770	856	17	RI def.1(20+), C-O str.(15+), C4C5 str.(15+), RI def.3(13+), C4N8 str.(12+)	

774	50	756	840	8	C4C5 str. (25+), CF str. (24+), RI def.1 (16−)	
772	30					MS
700	4	702	867	1	C-O OOPL wag. (47+), C4N8 OOPL wag. (36−)	
608	6					
600	8					
585		588	653	1	RI def.2 (32−), C-O bend. (15−),	
582	8				CF bend. (15−)	
565	36	516	637	365	NH_2 OOPL tor. (72−), CF OOPL wag. (11+)	
553	24	534	593	9	RI def.3 (28+), C4N8 bend. (21−), CO bend. (14−)	
550	14	452	558	116	OH OOPL wag. (91)	
542	16	460	569	65	NH_2 OOPL tor. (90+)	
487*	3*	486	540	3	RI def.2 (42−), CO bend. (10+), CF str. (10−)	
482*	2*					
446*	4*	426	526	70	RI OOPL def.3 (51−), RI OOPL def.1 (12−), NH_2 OOPL tor. (11+)	
373*	10*	354	438	0	CF OOPL wag. (76+)	
330*	10*					
317*	13*	343	381	13	CO bend. (45+), CF bend. (17−), C4N8 bend (13−)	
287*	7*	266	295	10	CF bend. (46−), C4N8 bend. (42+)	
253*	2*	212	262	12	RI def.3 OOPL (41−), RI def.1 OOPL (26+), C4N8 OOPL wag. (20−), CO OOPL wag. (12−)	
–**		132	163	1	RI OOPL def.2 (89)	

[a]Relative intensities at maximum expressed in relative units chosen in such a way that a sum of the intensities of all experimentally observed bands was supposed to be equal to a sum of the calculated intensities of all normal modes. *In N_2 matrix [24]; **below studied region. [b]Calculated frequencies scaled by the following factors: 0.92, OH stretch; 0.91, all other in-plane modes; 0.81, all out-of-plane modes. We have chosen these scaling factors on the basis of the following considerations: the scaling factor for the OH stretch follows from the comparison of the experimental matrix spectrum frequency and the calculated (3-21G) frequency of several hydroxypyrimidines. In the assignment of the absorption at 3602 cm^{-1} to the OH stretching mode, but not to the asymmetric stretching mode of NH_2 group, we have also taken into account the relative intensities of the asymmetric and symmetric stretching modes of the NH_2 group. It is well established that the ratio of the intensities A(assym)/A(sym) is of the order 0.6–0.7. Such a ratio of intensities is observed for the absorption bands near 3564 cm^{-1} and that near 3448 cm^{-1} $A(3564/A(3445)=82/116=0.7$. While the ratio of intensities $A(3602)/A(3445)=126/116=1.1$). Scaling factor 0.91, was used to achieve better agreement with the experimental frequencies of the stretching vibrations of the NH_2 group, for which the assignment was rather obvious. The same scaling factor, 0.91, was used for all other in-plane modes to obtain the best average agreement between the experimental and calculated spectra. A scaling factor of 0.81 was used for out-of-plane modes comparing the frequencies of the strong out-of-plane vibration in experimental spectrum, for which the assignment seems to be rather certain with the frequency of the strongest out-of-plane band being predicted by the calculation. [c]The potential-energy distribution (PED) was calculated according to the procedure described in ref. 23. The definitions of the symmetry coordinates are given in Table 2 and Fig. 2. [d]Abbreviations: str., stretch; sc., scissoring; ROT, rotational isomers; Ass, self-associated molecules; o, amino-oxo tautomer; MS, matrix splitting; FR, Fermi resonance; def., deformation; bend., bending; rock., rocking; OOPL, out-of-plane; wag., wagging; tor., torsion; sym., symmetric; asym., asymmetric, RI., ring, signs (+,−) describe phases of the motions.

with the spectrum calculated for the same tautomer is shown in Figs. 4(a) and 4(b). As seen there, the spectral patterns are generally similar for both spectra. However, on closer examination it can be seen in the experimental spectrum that many bands split into several more-or-less well-resolved components (with frequencies given in Table 5) which contribute to the total intensity in the spectral region under consideration, and which render the comparison of the experimental spectrum with the calculated frequencies and intensities not exactly straightforward. Such splitting could be due to: (i) matrix site effects (e.g. [18b,c,22]), leading often to the appearance of two or more sub-bands separated by a few wavenumbers (from 2 to 15 cm^{-1}); (ii) Fermi resonance between a fundamental mode and a nearby combination band involving lower-frequency modes of the appropriate symmetry. The second effect may produce multicomponent bands with splittings varying from 2 to 40 cm^{-1} and different relative intensities all of which arise primarily from the intensity of the unperturbed fundamental. Some of the weak bands could also possibly be due to traces of the amino-oxo tautomer or to self-associated dimers. However, these bands, if present, are expected to be very weak indeed, as indicated by the very low absorbance of the C=O stretching mode near 1700 cm^{-1} which has the largest molar absorption coefficient of all the IR absorption bands of the amino-oxo tautomer.

A comparison between the experimental spectrum and the calculated spectrum is complicated additionally by the fact that the matrix experiment does not give absolute values for the absorption intensities, but only relative values because the precise concentration and optical path length are not known. However, the relative experimental intensities given in Fig. 4(a) and Table 5 are normalized so that the sum of the intensities of all bands observed is equal to the sum of the calculated intensities for all the normal modes. As a result, such relative experimental intensities are more equivalent to the calculated intensities. As seen in Table 5, the calculated intensities agree with the experimental intensities for some of the normal modes, but for many normal modes the calculated and experimental intensities (the latter often consisting of several components) differ by a factor of 2 or 3. For some in-plane modes, particularly the very weak modes, and for most of the out-of-plane modes, the difference is even larger. It seems also that vibrations in the 1600–1200 cm^{-1} region are strongly coupled and that this coupling affects the experimental frequencies and relative intensities. However, taking into account all the complications involved in the experimental spectrum, and the relatively small basis set used for the calculation of the vibrational spectrum, we consider the agreement between the experimental and calculated spectra to be satisfactory. It is definitely helpful in the interpretation and understanding of the experimental IR spectrum of the isolated molecules to have the calculation available for comparison. Calculated molar absorption coefficients are useful in estimating the

TABLE 6

Vibrational frequencies, ν, IR intensities, A, and assignment of the absorption bands of isolated 5FC deuterated at ND2 and N1D

Experimental (Ar)		Calculation				Additional experimental bands; assignment[d]
ν (cm^{-1})	A (rel)[a]	ν^b (cm^{-1}) Scaled	ν^b (cm^{-1}) Unscaled	A (km mol^{-1})	PED[c]	
Not visible		3104	3411	4	C6H str. (99)	
2575	36	2670	2902	49	ND_2 assym.str. (100)	
2573	33					ROT, MS
2558	69	2643	2842	76	OD str. (100)	
2533	15					ROT, MS
2525	36	2516	2735	111	ND_2 symm.str. (98)	
2516	15					ROT,
2512	24					MS
2510	24					
1736	6					
1716	12					C=O/o,
1682	9					Ass
1636	27					o
1625	159	1628	1789	165	C5C6 str. (39 −), C6H bend. (13 +)	
1614	87					FR: e.g. 1140 + 478 = 1618
1612	90					MS,
1596	54					FR: e.g. 953 + 657 = 1610
1530	18					953 + 578 = 1531
1516	96					1140 + 392 = 1532
1514	100	1560	1712	330	C4C5 str. (32 −), N1C2 str. (21 −)	
1509	54					
1505	54					FR: e.g. 1192 + 326 = 1518
1498	39					MS,
1492	27					FR: e.g. 749 + 749 = 1498
						FR: e.g. 953 + 657 = 1610

TABLE 6 (continued)

Experimental (Ar)		Calculation				Additional experimental bands; assignment[d]
ν (cm^{-1})	A (rel)[a]	ν^b (cm^{-1}) Scaled	ν^b (cm^{-1}) Unscaled	A (km mol^{-1})	PED[c]	
1461	48	1512	1662	27	C4N8 str.(24+), N3C4 str.(17−), RI def.1(16−), C2N3 str.(16−), CO str.(15+)	
1447	141					FR: e.g. 953+508=1461
1443	29					MS,
1438	45					MS,
1432	51					FR: e.g. 953+478=1431
1425	189	1478	1624	946	C2N3 str.(16+), N3C4 str.(14−), CO str.(14−), N1C2 str.(12+), C4N8 str.(11+)	
1414	12					FR: e.g. 920+478=1398
1397	6					749+657=1406
1370	15					FR: e.g. 1140+249=1389
1361	24					MS
1360	27	1348	1481	3	C6H bend.(24−), N1C6 str.(19−), C5C6 str.(18−)	
1297	15					MS
1291	90	1290	1418	47	C6H bend.(30−), CO str.(15−), ND_2 sc.(13+), C4N8 str.(11+)	
1285	9					
1243	21					MS
1241	30	1256	1380	42	CF str.(23−), C6H bend.(17+), ND_2 sc.(15+), N3C4 str.(11+), RI def.1(11−)	
1230	15					
1228	15					MS
1224	30	1192	1296	12	ND_2 sc.(57+), RI def.1(11+)	
1140	63	1149	1262	96	N1C6 str.(34+), N1C2 str.(17−)	
1046	27	1025	1126	4	C2N3 str.(14+), ND_2 rock.(13+), OD bend.(13+), C4N8 str.(12−)	

1026	9				
956	42				
953	126	941	1023	161	OD bend.(55−), N1C2 str.(23+)
940	9				
936	12	938	1158	12	C6H OOPL wag.(100)
920	21	881	958	23	ND_2 rock.(37−), RI def.1(22−)
906	3				
786	39	781	964	140	RI def.1 OOPL(48+), C4N8 OOPL wag.(31+), CO OOPL wag.(18+)
763	9				
759	9				
749	18	760	836	12	C4C5 str.(27−), RI def.3(20−), C4N8 str.(13−)
729	6	701	886	1	CO OOPL wag.(47+), C4N8 OOPL wag.(36−)
	-**	657	811	5	CF str.(20−), ND_2 rock.(17−), RI def.1(16+), C4C5 str.(15−), CO str.(13+)
	-**	578	635		RI def. 2(31−), RI def.3(14−), CF bend.(13−)
	-**	457	564	52	RI def.3 OOPL (32+), ND_2 tor.(19+), CF OOPL wag.(14−), RI def.1 OOPL(13+)
	-**	508	558	6	RI def.3(38+),
	-**	478	525	8	RI def.2(37−), CO bend.(21+)
	-**	392	484	110	ND_2 tor.(32+), RI def.3 OOPL(27−), CF OOPL wag.(22−)
	-**	358	442	121	ND_2 tor.(50+), CF OOPL wag.(22−), OD OOPL wag.(12−)
	-**	333	411	35	OD OOPL wag.(82+), ND_2 tor.(13+)
	-**	314	388	0.1	ND_2 tor.(69+), CF OOPL wag.(25+)
	-**	326	359	11	CO bend.(44−), CF bend.(25+)
	-**	249	274	9	C4N8 bend.(51−), CF bend.(33+)
	-**	198	245	24	RI def.3 OOPL(37−), RI def.1 OOPL(23+), C4N8 OOPL wag.(21−), CO OOPL wag.(12−)
	-**	130	161	1	RI def.1 OOPL (89)

[a-d]See footnotes to Table 5.

tautomeric equilibrium constants and the differences in the energies of the amino-hydroxy and amino-oxo tautomers.

The experimental matrix spectrum of analogs of 5FC deuterated at the amino group and the ring nitrogens (and O–H) is shown in Fig. 4(c). The corresponding calculated spectrum of this molecule is presented in Fig. 4(d). As was the case for undeuterated 5FC, there is general agreement between the patterns of the experimental and calculated spectra.

The frequencies and intensities of all experimentally observed bands and all calculated normal modes for the deuterated 5FC are listed in Table 6. Examination of the data in Table 6 shows that there are indeed differences between the experimental and calculated spectra. These differences result from the same factors that influence the spectrum of the undeuterated molecule, as discussed previously.

Comparison of the IR spectra of matrix-isolated 5FC, 5BrC and 5IC

Because we did not perform calculations of the vibrational spectra of 5BrC and 5IC, and since such data do not exist in the available literature, the tentative interpretation of the vibrational spectra of 5BrC and 5IC was made by a comparison of their matrix spectra with those of 5FC and cytosine [6].

Besides the difference in the spectral region related to the OH, N1H and C=O stretches already discussed in relation to their tautomerism, cytosines with different halogen atoms attached at the C5 carbon also show different spectral patterns in other parts of their spectra. All these differences can be found by examining Tables 5 and 7, in which the frequencies and intensities of all bands observed in the matrix spectra of these cytosines are collected. The most pronounced differences are well visualized in Figs. 3 and 5 showing the matrix spectra of all the 5-halogenated cytosines discussed here.

A systematic shift to low frequency correlated with the size of the atom attached to C5 is observed for both the asymmetric and symmetric stretches of the NH_2 group (Fig. 3). This shift probably results from the intramolecular interaction between the NH_2 group and the halogen substituent, predicted also by our calculation for 5FC, as discussed above.

The spectra of 5FC, 5BrC and 5IC differ strongly in the region where the strongest absorption bands appear (1650–1400 cm^{-1}). One of the most pronounced differences in the spectra in this region is the appearance near 1550 cm^{-1} of a relatively intense triplet for 5BrC and doublet for 5IC, while for 5FC it seems probable that the corresponding absorption seems to be shifted to near 1500 cm^{-1}. The spectral patterns near 1650–1600, 1400–1450 and 1300 cm^{-1} are also quite different, probably due to the effect of halogen substitution on the NH_2 scissor and ring vibrations.

According to our calculated PEDs for 5FC, the C–F stretching vibration should appear near 1237 cm^{-1}. Taking into account the mass effect, we can

TABLE 7

Vibrational frequencies, ν, IR intensities, A, and preliminary assignments of the bands observed in the spectra of 5BrC and 5IC isolated in an argon matrix

5BrC		5IC		Assignment[b]
ν (cm^{-1})	A (rel)[a]	ν (cm^{-1})	A (rel)[a]	
3596	108	3594	70	OH str.
3555	54	3546	56	NH_2 assym.str.
3550	32	3540	26	ROT
3454	5	3452	8	N1H str.o
3441	13	3433	10	
3438	81	3430	56	NH_2 symm.str.
3434	45	3436	30	ROT
1778	5	1783	4	
1752	5	1750	10	FR/o
1730	5	1734	6	o/MS,
1724	49	1722	44	o/C=O str.
1718	9	1718	14	
1654	9	1652	12	
1648	22	1646	10	
1644	13			
1634	22	1636	6	
1629	90	1624	54	NH_2 sc.
1622	45	1620	100	C5C6 str.
1618	72	1610	46	
1609	90	1620	100	C5=C6 str.
1606	198	1698	70	
1588	13	1584	10	
1578	9	1580	10	
1575	7	1576	10	
1568	54	1562	60	RI str. FR, MS
1562	90	1558	26	
1656	54	1550	100	
1527	5	1522	3	
1516	5	1514	10	
1507	5	1508	6	
		1506	8	
1478	22	1470	16	
1475	31	1468	22	
1472	13	1464	12	
1442	252	1438	230	RI str., RI def., C-O str.
1437	36			FR, MS
1434	63	1430	64	
1430	27			
1424	36			
1420	67	1428	130	RI str.,
1418	54	1413	50	C_4N_8 str.

TABLE 7 (continued)

5BrC		5IC		Assignment[b]
ν (cm^{-1})	A (rel)[a]	ν (cm^{-1})	A (rel)[a]	
1363	17	1359	10	RI str., C6H bend., OH bend.
1350	180	1345	144	C_6H bend, OH bend.
1343	5	1339	4	
1337	3	1331	2	
1306	3			
1300	7	1300	10	
1296	25			
1286	3			
1258	27	1258	32	
1242	3	1246	2	
1234	3	1234	6	
1220	8	1225	6	
1202	32	1203	20	
1190	65	1190	94	OH bend., RI str., NH_2 rock.
1178	3	1178	4	RI str.
1171	3	1162	2	
1088	94	1088	56	NH_2 rock., RI str., OH bend.
1055	22			CBr str.
		1037	18	CI str.
976	7	976	8	RI str., RI def., NH_2 rock.
954	3	956	2	
950	7	953	4	C6H OOPL wag.
789	45	790	30	RI def. OOPL
779	9	779	5	RI str., RI def., C-O str.
773	5	774	4	
652	9			CBr str., RI str., RI def.
		637	8	CI str., RI str., RI def.
611	31			
		614	4	
605	11	604	12	
601	9			
590	5	570	3	RI def., C-O bend.
558	5	566	4	
545	9			
530	14	528	10	NH OOPL tor.
526	5			
518	27	516	30	OH OOPL wag.
515	22	511	40	
509	27	508	18	

[a]See footnote a to Table 5. [b]See footnotes c and d to Table 5.

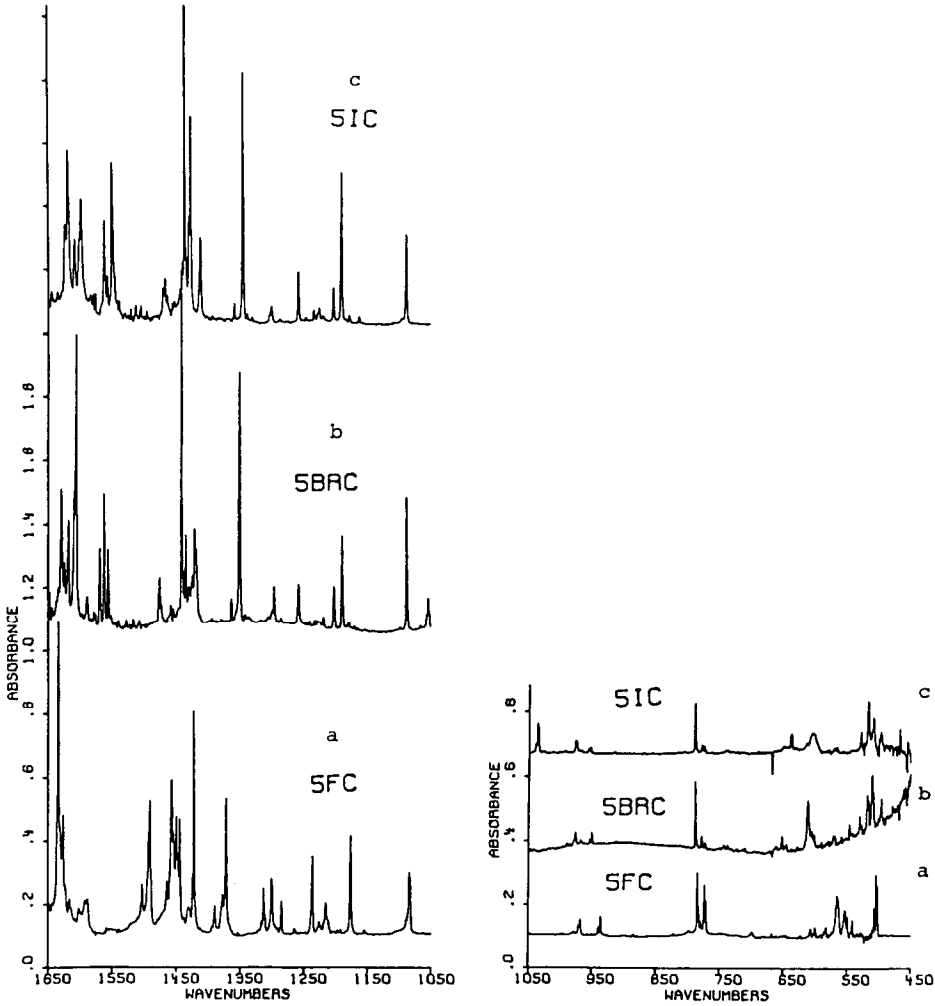

Fig. 5. Comparison of the IR spectra in the 1650-450 cm^{-1} region of 5FC (a), 5BrC (b) and 5IC (c) each isolated in an argon matrix at about 15 K.

expect that the C–Br and C–I stretches should be shifted down to about 1000 cm^{-1}. This suggests that the absorption band observed at 1055 cm^{-1} exclusively in the spectrum of 5BrC is probably related to the C–Br stretch, and the band at 1035 cm^{-1}, which appears only in the spectrum of 5IC, is related to the C–I stretch.

Similar comparison and estimation suggests that other absorption bands related to the in-plane stretching motions of the C–F, C–Br and C–I bonds are located at 774 cm^{-1} for 5FC, at 650 cm^{-1} for 5BrC and at 637 cm^{-1} for 5IC.

The out-of-plane bending vibrations of the CBr and CI groups are expected to appear at wavenumbers below the studied region.

The interpretation of the vibrational spectra of 5BrC and 5IC proposed in Table 7 is more uncertain than is that for cytosine [6] and 5FC, and it must be considered as very tentative. It is expected that improved assignments may be possible when quantum mechanical calculations of the vibrational spectra with good basis sets (possibly better than that used for the calculation of the spectra of 5FC and cytosine) become available.

Amino-oxo tautomer in the crystalline solid

As has been shown before, 5FC and other 5-halogenated cytosines when isolated in an inert matrix exist predominantly in the amino-hydroxy form with only a small amount of the amino-oxo form present. Hence in the matrix spectrum only the strongest absorption bands of the amino-oxo form (mainly C=O stretch) can be detected. The calculated spectrum of the amino-oxo tautomer of 5FC must be compared, therefore, with the spectrum of the crystalline solid, where this tautomer is exclusively present. Figure 6 and Table 8 show such a comparison of the experimental IR and Raman spectra of the crystalline solid 5FC sample with the calculated IR and Raman spectra of the amino-oxo tautomer. The spectra of crystalline 5BrC and 5IC (not discussed here) prove that these molecules also exist in the crystal in the amino-oxo form. Because molecules in the crystal are involved in hydrogen bonding and other intermolecular interactions but the spectrum is calculated for non-interacting isolated molecules, we can expect that the agreement between the experimental and calculated spectra will be worse than for the case of the amino-hydroxy tautomer of 5FC isolated in an argon matrix which was previously discussed. Hydrogen bonding is expected to change most drastically the stretching and bending vibrations of the N1H and NH_2 groups. It usually has much less effect on the vibrations of the C=O group and even less on the vibrations of the ring or of the CH group. Nevertheless the calculations provide some help in the interpretation of the spectrum of the crystalline solid. The details of the comparison of the experimental and calculated spectra for crystalline 5FC are given in Table 8. The differences in the spectrum of molecules in crystalline solid (in oxo form) and those isolated in an argon matrix (in hydroxy form) can be seen by comparing relative absorption bands listed in Table 8 with those in Table 5.

It should be noted that the calculated Raman intensities are in much worse agreement with those observed experimentally than are the calculated intensities for the IR spectrum. This suggests that the calculation with the GAUSSIAN 86 program using a 3-21G basis set is not good enough for useful prediction of Raman intensities.

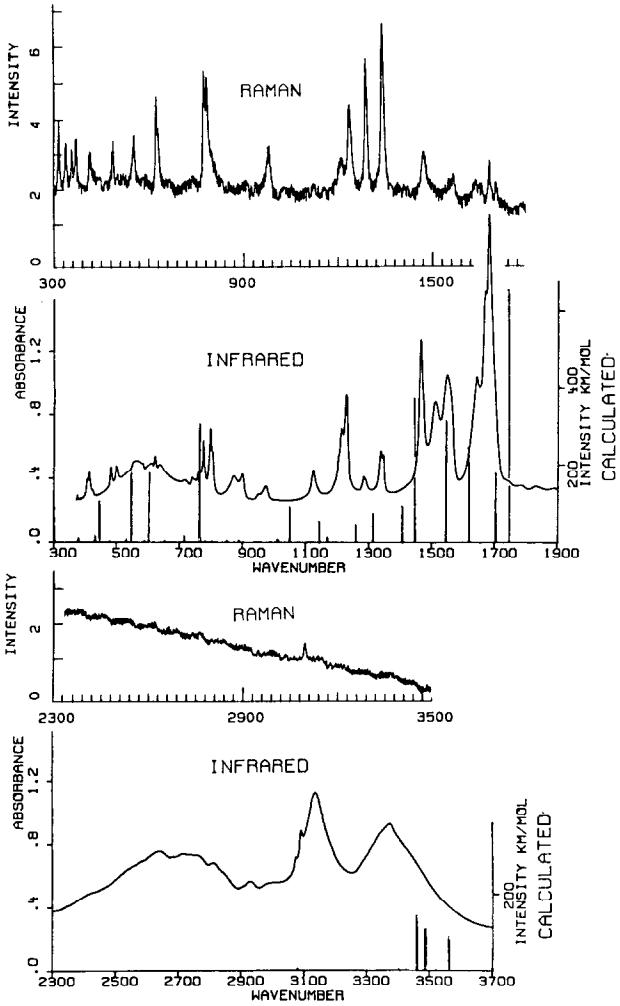

Fig. 6. Comparison of the IR (in KBr pellet) and Raman (in capillary tube) spectra of 5FC crystalline solid samples. Vertical lines show the calculated IR spectrum of the amino-oxo form. Raman spectra of the powdered samples were measured using a Spex Model 1701 double monochromator (slits 350 μm) with a cooled photomultiplier (RCA 3130) in the photon-counting mode. Excitation was via the 514-nm line (100 mW) of an Ar^+ laser (Spectra-Physics 2000 Series). Interfering plasma lines were practically eliminated with a laboratory-made prism prefilter. The sample, contained in a vertically oriented capillary tube, was rapidly rotated during irradiation; the scattered radiation was collected in a 180° back-scatter orientation. A microcomputer (HP 3000) controlled the wavenumber advance, the signal averaging and the spectral display, storage and recording.

TABLE 8

Comparison of the experimental IR and Raman spectra frequencies, ν, and intensities A (IR) and I (Raman) of crystalline 5FC with the calculated spectra of the amino-oxo tautomer

Experiment				Calculation				PED[d]
IR		Raman		ν^c (cm^{-1})		A	I	
ν (cm^{-1})	A (rel)[a]	ν (cm^{-1})	I (rel)[b]	Scaled	Unscaled	IR (km mol^{-1})	Raman (Å^4 amu^{-1})	
3370	~1700			3560	3913	95	56	NH_2 assym.str.(100)
3136	~1000			3405	3783	139	105	NH_2 symm.str.(100)
3091	32	3088	3	3115	3424	1	79	C6H str.(99)
3073	sh							
2990	40							
2927	28							
2690	~2500			3468	3811	113	95	N1H str.(100)
		1703	4					
1684	458			1642	1804	247	14	NH_2 sc.(91)
1672	336	1671	8	1775	1951	658	17	C=O str.(72−)
1644	200	1631	5	1724	1895	180	16	C5C6 str.(54+), C6H bend.(10−)
1550	400	1556	5	1568	1723	349	24	N3C4 str.(48+), N1H bend.(11−)
1512	320			1426	1567	92	12	N1H bend.(50−), C4C5 str.(11+)
1467	225	1465	8	1472	1618	378	9	C4N8 str.(26+), C4C5 str.(21−), N1H bend.(10−)
1346	72							
1339	80	1334	25	1332	1464	71	12	C6H bend.(54−)
1287	40	1281	20	1283	1410	46	1	CF str.(26−), RI def.1(18−), C4N8 str.(17+)
1229	168	1228	14	1163	1278	64	5	N1C2 str. (54+), N1H bend.(14+), C6H bend.(12−), N1C2 str.(11−)
1214	116			1062	1167	90	5	NH_2 rock.(24+), N1C2 str.(18+), C2N2 str.(16−), C–O bend.(15−)
		1202	6					
1125	48			1148	1302	16	9	NH_2 rock.(32+), C2N3 str.(23+), CF str.(11−)
974	24	973	7	916	1167	6	5	C6H OOPL wag.(100)

951	12							
899	44			894	983	8	3	N1C2 str.(25+), RI def.1(22−), C4C5 str.(14−), C2N3 str.(11+)
			873	40				
802	sh							
797	116	777	16	773	954	290	5	C=O OOPL wag.(49+), RI def.1 OOPL(23+), C4N8 OOPL wag.(18+), N1H OOPL wag.(10+)
775	100	768	17	791	870	5	4	RI def.1(38−), CF str.(16+), N1C2 str.(15−)
				733	905	0	3	C4N8 OOPL wag.(46+), C=O OOPL wag.(29−), N1H OOPL wag.(14−)
717	4			722	794	17	113	C4C5 str.(38+), RI def.3(11+), N1C2 str.(10+)
636	4			600	660	2	6	C=O bend.(30−), CF bend.(20−), RI def.2(10−)
622	~120	623	9	598	739	174	2	N1H OOPL wag.(77+)
611	~300	618	13	548	677	180	5	NH_2 tor.(80+)
		546	8	536	589	0.4	3	RI def.3(34+), RI def.2(18+), C4N8 bend.(16−), C=O bend.(12−)
565	~340			477	589	105	3	NH_2tor.(95+)
500	28							
482	32	479	7	485	534	2	4	RI def.2(46−), RI def.3(25+)
413	48	405	6	390	482	17	2	RI def.300PL(58+)
408	sh							
		362	7	376	413	9	1	C=O bend.(26+), CF bend.(21−), C4N8 bend.(20−)
		329	7	323	399	1	2	C-F OOPL wag.(92)
		307	10	280	308	8	4	CF bend.(47−), C4N8 bend.(37+)
		227	2	197	243	10	0.2	RI def.3 OOPL(42−), RI def.1 OOPL(37+), C4N8 OOPL wag.(13−)
		121	34	108	133	12	0.5	RI def.2 OOPL(100)
		88	60					
		69	51	Libration, translation, and hydrogen bond intermolecular vibrations[e]				
		63	46					
		55	33					

[a]See footnote a to Table 5; with the exception of the intensities of NH_2 stretching and torsion and N1H stretching and wagging motions for which the maximum intensities were multiplied by a factor related to the differencee in the widths of these modes and other modes in the spectrum of crystalline solid. [b]See footnote a to Table 5. [c]Calculated frequencies scaled by the following factors: 0.91, all in-plane modes; 0.81, all out-of-plane modes (see also footnote b to Table 5). [d]See footnote c to Table 5. [e]See results for 1-methyluracil single crystal studies by Colombo and Kirin [25].

CONCLUSIONS

The amino-hydroxy tautomer of 5FC, 5BrC and 5IC dominates when these molecules are isolated in an inert environment, in sharp contrast to the exclusive appearance of the amino-oxo tautomer in polar environments.

The ab initio calculation of energy at the HF level (6-31G**//3-21G) performed for 5FC also predicts that the amino-hydroxy tautomer is more stable. The calculated energy difference [E(amino-hydroxy) $-E$(amino-oxo) $= -13$ kJ mol^{-1}] is surprisingly close to the experimentally estimated enthalpy difference in the vapor phase at 500 K ($\Delta K = -13 \pm 2$ kJ mol^{-1}). The higher stability of the amino-oxo tautomer of 5FC in the polar environment is apparently correlated with the largest dipole moment for this tautomer.

The experimentally determined equilibrium constant, K(h/o), and the enthalpy difference from amino-hydroxy and amino-oxo tautomers gradually increases in going from cytosine to 5IC, to 5BrC to 5FC. This order correlates with the increasing electronegativity of halogen atoms.

The calculation (3-21G) of the vibrational frequencies and intensities provided useful data for interpretation of the experimental IR spectra of 5FC.

By comparison of the IR matrix spectrum of 5FC with those of 5BrC and 5IC a tentative interpretation of the matrix spectra of these two molecules is proposed.

The IR spectrum of the amino-oxo tautomer, which dominates in the crystalline sample, was interpreted by comparison with the calculated IR spectrum of this tautomer. This comparison allows us to determine changes in the frequencies and intensities due to intermolecular interactions, particularly hydrogen bonding, in the crystal.

ACKNOWLEDGEMENT

Support for this work was provided by NIH Research Grant No. GM-32988, and is gratefully acknowledged. The authors wish to thank Professor J.S. Kwiatkowski, Dr.E. Kulikowska and Dr. L. Adamowicz for many valuable discussions. A.J. wishes also to acknowledge support from the Ministry of Science and Higher Education (Poland) within the project CPBP 8.14. We are also very grateful to the Pittsburg Superconductor center for computing support (under PSCA Grant CHE-8700 42 P).

REFERENCES

1 (a) J. Malbica, L. Sello, B. Tabenkin, J. Berger, E. Grunberg, J.H. Burchenal, J.J. Fox, I. Wempen, T. Gabriel and R. Duschinsky, Fed. Proc., 21 (1962) 384.
(b) E. Grunberg, E. Titsworth and M. Bennet, Antimicrob. Agents Chemother., 1963 (1962) 566.
(c) J.E. Bennett, N. Engl., J. Med., 290 (1974) 30.

2 R. Duschinsky, T. Gabriel, M. Hoffer, J. Berger, E. Titsworth, E. Grunberg, J.H. Burchenal and J.J. Fox, J. Med. Chem., 9 (1966) 566.
3 J.H. Burchenal, V.E. Currie, M.D. Dowling, J.J. Fox and I.H. Krakoff, Ann. N.Y. Acad. Sci., 255 (1975) 202.
4 (a) A. Polak, Ann. Biol. Chim. (Paris), 45 (1987) 669, and references therein.
(b) E. DeClercq, J. Beres, W.G. Bentrude, Mol. Pharmacol., 32 (1987) 286.
(c) P. Brasseur, G. Bonmarchard, F. Caron, F. Lecomte, J. Leroy and G. Humbert, Ann. Biol. Chim. (Paris), 45 (1987) 685.
5 (a) K.A. Hartman, R.C. Lord and G.J. Thomas, Jr., in Physico-Chemical Properties of Nucleic Acid Bases, Vol. 2, Academic Press, London, 1983, Chap. 10.
(b) M. Tsubi, S. Takahasi and I. Harada, in Physico-Chemical Properties of Nucleic Acid Bases, Vol. 2, Academic Press, London, 1983, Chap. 11.
(c) R.J.H. Clark and R.E. Hester (Eds.), Advances in Spectroscopy, Vol. 13, Spectroscopy of Biological Systems, Wiley, Chichester, 1986.
(d) E. Taillandier, J. Liquier and J.A. Taboury, in R.J.H. Clark and R.E. Hester (Eds.), Advances in Infrared and Raman Spectroscopy, Vol. 12, Wiley, Chichester, 1985, Chap. 2.
6 M. Szczesniak, K. Szczepaniak, J.S. Kwiatkowski, K. KuBulat and W.B. Person, J. Am. Chem. Soc., 110 (1988) 8319.
7 M. Szczesniak, M.J. Nowak, H. Rostkowska, K. Szczepaniak, W.B. Person and D. Shugar, J. Am. Chem. Soc., 105 (1983) 5969.
8 (a) J.S. Binkley, J.A. Pople and W.J. Hehre, J. Am. Chem. Soc., 102 (1980) 939.
(b) M. Dupuis, D. Spangler, J.J. Wendolowski, NRCC Software Catalog, University of California, Berkeley, CA, 1980, Program QG01.
(c) M.W. Schmidt, J.A. Boatz, K.K. Baldridge, S. Kosecki, M.S. Gordon, S.T. Elbert and B. Lam, Q.C.P.E. Bull., s17 (1987) 115.
(d) J.S. Binkley, M.J. Frish, D.J. DeFrees, K. Raghavachari, R.A. Whiteside, H.B. Shlegel, E.M. Fluder and A.J. Pople, GAUSSIAN 82, Carnegie-Mellon University, Pittsburgh, PA, 1983.
(e) M.J. Scanlan and I.H. Hillier, J. Am. Chem. Soc., 106 (1984) 3737.
(f) P.C. Hariharan and J.A. Pople, Chem. Phys. Lett., 66 (1972) 217.
(g) M.M. Francl, W.J. Pietro, W.J. Hehre, J.S. Brinkley, M.S. Gordon, D.J. DeFrees and A.J. Pople, J. Chem. Phys., 77 (1982) 3654.
9 (a) Ch.E. Bugg and H. Sternglanz, Jerusalem Symp., 7 (1974) 473.
(b) T. Kulikowski and D. Shugar, Acta Biochim. Polon., 26 (1979) 145.
10 J.S. Kwiatkowski, R.J. Bartlett and W.B. Person, J. Am. Chem. Soc., 110 (1988) 2353.
11 A. Les, L. Adamowicz and R.J. Bartlett, J. Phys. Chem., 93 (1990) 4001.
12 L. Adamowicz and R.J. Bartlett, J. Chem. Phys., 86 (1987) 6314.
13 J.S. Kwiatkowski, W.B. Person, K. Szczepaniak and M. Szczesniak, Acta Biochim. Polon., 34 (1987) 165.
14 G. Fogarasi and P. Pulay, J. Mol. Struct., 39 (1977) 275.
15 (a) P. Pulay, G. Fogarasi, G. Pongor, J.E. Boogs and A. Vargha, J. Am. Chem. Soc., 105 (1983) 7037.
(b) B. Fagarasi and P. Pulay, Ann. Rev. Phys. Chem., 35 (1984) 191.
(c) P. Botschwina, Chem. Phys. Lett., 29 (1974) 98.
(d) C.E. Blom and C. Altona, Mol. Phys., 31 (1976) 1377.
16 L. Lapinski, R. Czerminski, M.J. Nowak and J. Fulara, J. Mol. Struct., in press.
17 (a) R. Czerminski, K. Kuczera, H. Rostkowska, M.J. Nowak and K. Szczepaniak, J. Mol. Struct., 140 (1986) 235.
(b) M.J. Nowak, K. Szczepaniak, A. Barski and D. Shugar, J. Mol. Struct., 62 (1980) 47.
18 (a) M.J. Nowak, K. Szczepaniak, A. Barski and D. Shugar, Z. Naturforsch. Teil C, 33 (1978) 876.

(b) M. Szczesniak, M.J. Nowak, H. Rostkowska, K. Szczepaniak, W.B. Person and D. Shugar, J. Am. Chem. Soc., 105 (1983) 5969.
(c) M. Szczesniak, M.J. Nowak, K. Szczepaniak, S. Chin, I. Scott and W.B. Person, Spectrochim. Acta, Part A, 41 (1985) 223.
19 R. Czerminski, J.S. Kwiatkowski, W.B. Person and K. Szczepaniak, J. Mol. Struct., 198 (1989) 297.
20 C.A. Coulson, Valence, Oxford University Press, London, 1961, p. 140.
21 L. Adamowicz, Chem. Phys. Lett., 153 (1988) 147.
22 (a) H.E. Hallam (Ed.), Vibrational Spectroscopy of Trapped Species, Wiley, London, 1973.
(b) A.J. Barnes, in W.J. Orville-Thomas, A. Muller, R. Gaufries (Eds.), Matrix Isolation Spectroscopy, Riedel, Dordrecht, 1981.
23 (a) Y. Morino and K. Kuchitsu, J. Chem. Phys., 20 (1952) 1809.
(b) G. Keresztury and G. Jalsovsky, J. Mol. Struct., 10 (1971) 304.
24 (a) M. Szczesniak, Ph.D. Thesis, Institute of Physics, Polish Academy of Sciences, Warsaw, 1985.
(b) K. Kuczera, M. Szczesniak and K. Szczepaniak, J. Mol. Struct., 172 (1988) 89.
25 L. Colombo and D. Kiri, Spectrochim. Acta, Part A, 42 (1986) 557.